

Fire Risk Monitoring and Assessment in British Columbia using Remote Sensing Concepts

FINAL REPORT

Anmol Saini & Kiana Lim

ahsaini@sfu.ca & kianal@sfu.ca

Department of Geography, Simon Fraser University

GEOG 453 - November 2022

Prepared for: Dr. Bing Lu & Lilian Yang

Abstract

British Columbians and local wildlife benefit from forests because they offer both economic and environmental advantages. Forest fires are becoming increasingly extreme in terms of duration, cost of recovery, and frequency due to climate change and human activity. Recent forest fires in British Columbia have had a negative impact on ecosystems, forced communities to relocate, and harmed people's health. The purpose of this project is to develop a method for estimating the burn intensity of recent forest fires and to track trends in a selection of fire risk factors. Remote sensing data and methods were utilized to map fire-afflicted forests and assess a subset of variables for fire risk.

Input data for quantitative analysis used remotely sensed forest cover data, such as satellite optical images and digital elevation maps. Models and algorithms derived from a literature study were used alongside remote sensing software to assess the severity of burns and the frequency of fire risk factors using three study fires from three different years in BC.

This project provided preliminary remote sensing methods for examining burn severity and fire risk variables. Findings support current remote sensing literature stating that warmer temperatures, drier vegetation, and sloped topography are associated with higher wildfire risk. The project also adds to literature that exemplifies how remote sensing can be used for forest fire analysis. The results may guide provincial aerial fire management.

1. Introduction

In the last few decades, BC's forests have become vulnerable to wildfires with unprecedented duration, size, intensity, and costs. In both 2017 and 2018, there were declared states of emergency, and each year, more than one million acres burned (British Columbia, n.d.). Recent studies indicate that climate change may eventually result in an increase in the incidence and duration of forest fires (Wang et al., 2015). Despite the fact that fire cycles are a naturally occurring process, human activity has stifled them, which has an impact on other natural cycles, habitations, air quality, and the economy (Rittmaster et al., 2006; Schoennagel et al., 2017).

The association between wildfires and climate change discussed above has been observed in places outside of British Columbia (White et al., 2017; Haider et al., 2019). Thus, there is a significant number of remote sensing literature available, regardless of the study region, as a result of the substantial effects that wildfires have on the built and natural environment. It is advantageous to use remote sensing to monitor risky and fire-affected areas because it can help institutions make decisions regarding disaster preparedness, environmental management, conservation, and economic and environmental recovery (Leblon et al., 2012; White et al., 2017; Filippioni, 2019). As previously mentioned, forest fires can be strong and destructive dangers at several geographical scales, thus anticipating and evaluating contributing elements is crucial.

In order to forecast probable fires, the remote sensing study monitored specific BC woods and evaluated pre- and post-fire characteristics. Findings raised awareness of the causes of forest fires. The findings offered a basic foundation for identifying and forecasting fire-risk areas in British Columbia. This initiative could assist provincial fire management agencies in properly allocating their fire prevention resources in order to conserve current forest cover and lessen any negative effects on the economy and public health that may result. Lastly, this initiative will

contribute to the sparse literature on how remote sensing can be used to manage and monitor forest fires in British Columbia. The project will fill a research gap by evaluating recent fires in the past five years, in south-central and south-eastern British Columbia on a finer spatial scale.

2. Methodology

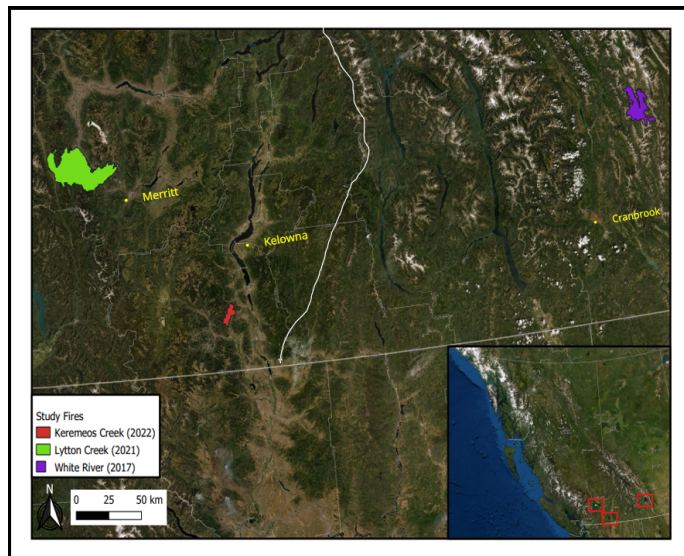
2.1. Study area

Three different forest fire sites within southern BC were chosen as study areas. The first study fire is White River which ignited on July 29th, 2017, followed by Lytton Creek, which began on June 30th, 2021, and Keremeos Creek, which started on July 29th, 2022. Fires were chosen based on recency, magnitude, and data accessibility. Due to relatively weaker fire seasons in 2019 and 2020 and a lack of precise data for fires in 2018, the first study area is from 2017.

White River is located in the BC's Wildfire Service's Southeast fire center region. This region is bordered by the United States to the south, the Monashee Mountains (west), the Mica Dam (north), and Alberta (east). The Southeast region has a moist climate in the north, whereas the southwest Okanagan area has a dry desert environment. Mountainous topography leads to sweltering summers and freezing winters. This area contains a variety of economically valuable tree species (BC Wildfire Service, n.d.).

Within the Kamloops region (located east of the Southeast wildfire region) are the Lytton Creek and Keremeos Creek study fires. The area is bordered to the south by the United States, to the north by Blue River, to the west by Bridge River, and to the east by the Monashee Mountains (east). These areas include a variety of climates, including chilly glacial regions, semi-arid deserts, and rainforest regions. The resulting vegetation ranges from deciduous trees to desert plants (BC Wildfire Service, n.d.). The map below depicts the geographical location of the three forest fires within the scope of South British Columbia.

Figure 1. Map showing the three study areas situated in Southern BC, with an inset map showing all of BC.



2.2. Data collection methods

All data was collected from free, open-source databases. The Open Data Catalogue for BC was used to gather shapefile information for each fire. The Copernicus Open Access Hub and USGS EarthExplorer were used as sources for the optical, visual, and thermal remote sensing images. Sentinel-2, Landsat 8 and 9, and other satellites' images were gathered before, during, and after each of the three fire occurrences.

Images with a 0–10% cloud cover were chosen to avoid additional processing. Landsat and Sentinel were chosen due to

their availability of the desired bands such as the thermal data layer, moderate to higher spatial scale, and relative availability of study fire images. The literature study and earlier remote sensing course materials are where methodologies (i.e., particular computations) are found. Online tutorials, provincial websites, our literature review, and other peer-reviewed publications provided additional non-remote sensing data on historical wildfire averages, socioeconomic impacts, and other contextual information.

2.3. Data analysis

2.3.1. Post Fire Detection

The first step in data processing analyzed the extent and impact of the burned areas by calculating the normalized burn ratio (NBR) before and after the fire, and the associated burn severity. *NBR* is the ratio of near-infrared (NIR) and shortwave-infrared (SWIR2) values, which outlines burnt swaths of land (Alcaras et al., 2022). The NBR formula to be used:

$$NBR = \frac{(NIR - SWIR_2)}{(NIR + SWIR_2)} \quad (1)$$

The dNBR formula used in the interest of the Burn Severity maps:

$$dNBR = {}_{pre}NBR - {}_{post}NBR \quad (2)$$

To start, we used the bands 8A (NIR) and 12 (SWIR) from Sentinel 2 as inputs. Band 8A is a subset of Band 8. It was used because of its finer spectral range and its spatial resolution, which is identical to Band 12 (20m) and makes band calculations simple. Two sets of Band 8A and 12 images were gathered - one for a pre-fire date, and another for a post-fire date. These bands were used because they are sensitive to changes in vegetation. The main steps to generate the NBR and dNBR products consisted of:

- i. Clipping each raster layer to the perimeters of each fire area.
- ii. Normalizing all the clipped layers to a 0 to 1 scale, to assure results are proportional.
- iii. Computing NBR from formula (1) where band 8A is NIR and band 12 is SWIR2.
- iv. Calculating dNBR by subtracting post-fire NBR from pre-fire NBR.

Various geoprocessing tools from QGIS were used to execute these steps, which were all organized within a custom-created Graphical Modeler. This was to ensure that the same precise steps were taken for computing NBR products for the three different fire study areas. Figure 5 in the Appendix displays the graphical modeler with the steps to produce the NBR maps.

The next analysis step used NBR to calculate *burn severity*. Burn severity quantifies and visualizes wildfire burned areas within a designated study area. For each fire, we subtracted the NBR values for each pre and post fire image. Resulting dNBR raster values were rescaled to values of 0-1 for visual clarity. These calculations quantitatively measure forest cover loss, identify affected areas, and generate useful burn severity map products. The table below depicts the different burned area classification bins, used by the Government of BC (Burt, 2015). In our maps, higher dNBR values indicated stronger changes before and after each fire, following the same approach as multiple studies reviewed and cross-examined with many existing Burn Severity products publicly available online such as in the publication by Santos et al. (2020).

Classification Label	Pixels Range	Pixel Colors
Unburned	0 - 0.29	Green
Low Severity	0.29 - 0.43	Yellow
Medium Severity	0.43 - 0.70	Orange
High Severity	0.7 - 1	Dark Red

Table 1. Burned Severity classification levels as implemented by the BC Government.

2.3.2. Assessing Fire Risk Variables

The second part of analysis assessed *variables for fire risk*. In this study, land surface temperature (LST), fuel moisture, and slope are analyzed. Due to the team's limited expertise in the field and limited open-source data available, no further variables were observed. Each variable was examined before, during, and after each fire incident to recognize potential patterns. Comparing variables between each fire identifies pre-fire conditions that may indicate higher risk; additionally, comparing variables for each year will indicate potential trends to note in future years.

To compute the Land Surface Temperature of the pre-fire dates for each of the three study areas, the Semi-automatic Classification Plugin (SCP) in QGIS was used. The SCP performed atmospheric correction on the Landsat 8 and Landsat 9 bands, then converted the thermal bands of Landsat (Band 10) to brightness temperature in Celsius which provided a good estimate of LST. Figure 6 captures the view of how the SCP was used in QGIS. Furthermore, to understand the relationship between LST and hill sloping, the method in Adelabu et al. (2020) was followed, by using a digital elevation model (DEM) to assess topographic data overlaid on the land surface temperature data layers.

To forecast conditions that may increase wildfire likelihood, fuel moisture conditions were assessed on 3 pre-fire dates for each of the three fire incidents. Methods from Adelabu et al. (2020) were used to calculate the Fuel Moisture Index (FMI). Their FMI uses two other indices, Normalized Moisture Drought Index (NMDI) and Relative Greenness Index (RGI), as inputs. NMDI is useful for monitoring vegetation water content and stress (EOS, 2022). RGI compares the vegetation health (greenness) of a pixel over the entire range of green pixels over the time period (Schneider et al., 2008) and is the product of standardizing the Normalized Difference Water Index (NDWI). These two indices together contextualize weather conditions and the direction of forest fire spread. The specific formulas used to analyze the fuel moisture content include the following:

$$NDWI = \frac{(NIR - SWIR_2)}{(NIR + SWIR_2)} \quad (3)$$

$$RGI = \frac{(NDWI - NDWI_{min})}{(NDWI_{max} - NDWI_{min})} \times 100 \quad (4)$$

$$NMDI = \frac{(NIR - (SWIR_1 - SWIR_2))}{(NIR + (SWIR_1 + SWIR_2))} \quad (5)$$

$$FMI = \frac{(RGI - NMDI)}{NMDI} \quad (6)$$

The FMI processing requires 3 bands from Sentinel 2 where band 8A represents NIR, SWIR1 is equivalent to band 11 and SWIR2 is band 12. Seeing as the three raster bands are loaded into multiple formulas for each of the total of nine different dates that need to be processed and compared, another custom made model is made using QGIS' graphical modeler. The model is designed to calculate the formulas above in a concise and convenient manner, as can be seen in Figure 7 in the Appendix.

3. Results & Discussion

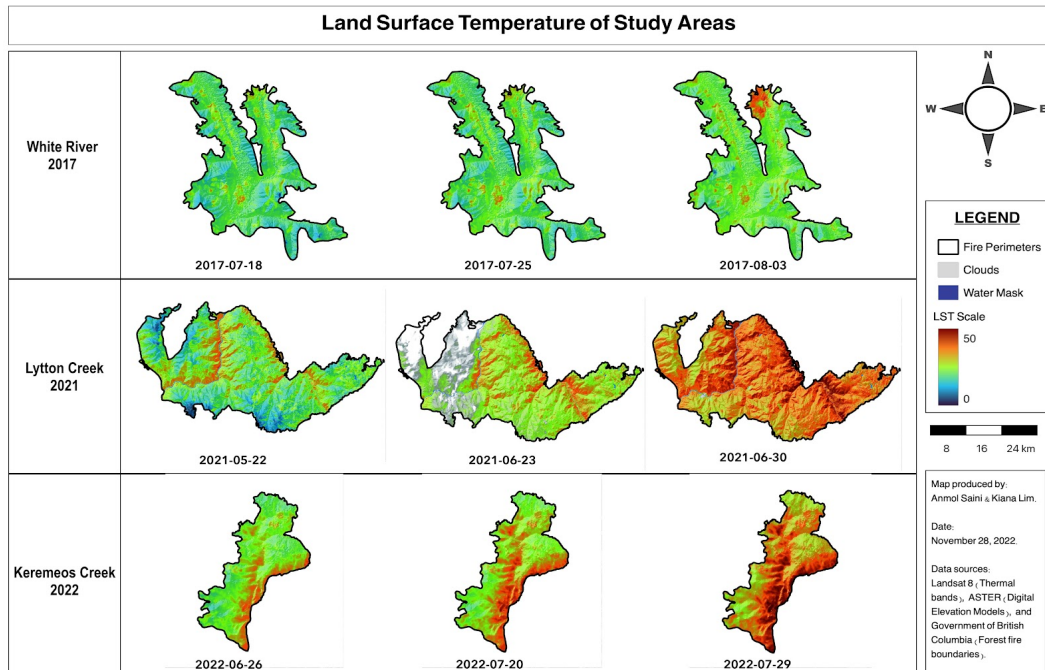
3.1. Qualitative analysis and histograms

Qualitative analysis for each collection of maps were supplemented with histograms to understand the distribution of wildfire variables. Histograms were generated in ArcGIS (see appendix graph sets 1-3). The digital elevation model was overlaid over land surface temperature, fuel moisture index, and burn severity maps to better understand the role of slope in wildfire variable risk.

3.1.1. LST and Slope

The final Land Surface Temperature map is shown in figure 2 below, which covers the pre-fire dates for each of the three fires. As can be seen in the image, the red pixels increased in all three fires, suggesting a warming trend leading up to each fire incident. Lytton Creek had some cloud cover on the imagery from June 23rd, 2022 that could have compromised results, however, the increase in LST over the region from the previous date is quite noticeable. Qualitative analysis exhibits the redder pixels occurred on the leeward slopes with warmer temperatures, and at lower altitudes.

Figure 2. LST of the three study areas on the pre-fire dates.



Histograms for each date LST were generated, which can be seen (see appendix - graph set 1) These histograms support the qualitative observations as the bars shifted right. The mean temperature increased slightly over each year's histogram set, further implying a warming trend leading up to the fire.

3.1.2. Fuel Moisture and Slope

Fuel moisture and slope results were more variable than expected, as noted from figure 3 below. White River and Lytton appeared drier before the fire, but some areas of Keremeos Creek experienced moisture conditions before the fire incident. This could be attributed to local weather patterns, as Keremeos Creek contains more water bodies in a smaller area. Additionally, the patches of red that indicate dry areas coincide with the source of each fire incident. Like LST, the fires originated in drier, leeward slopes and low latitude areas.

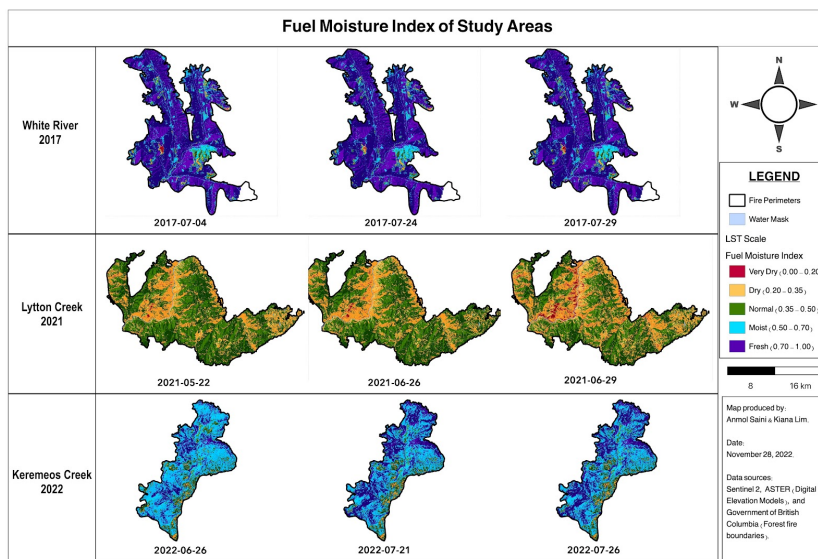


Figure 3. Fuel Moisture Index maps for pre-fire dates.

As can be seen from the image, the general color scheme (pixel range) of each study area is distinct even though all the maps are classified to the same FMI scale. This may be due to the variations in each regions atmospheric conditions, weather patterns, terrain, and time and duration of the fires. While we attempted to minimize the gap in data disparity to keep analysis consistent enough so patterns

can be recognized, unexpected elements of nature are inevitable.

The histograms in the appendix (graph set 2) indicate a slight decreasing trend for each study fire. The moisture decline was most evident in Lytton Creek. For White River and Keremeos Creek, the fuel moisture content of the overall area was marginally drier a month before the start of the fire. The FMI in both these regions then increased a week prior, then decreased once again around the ignition date. However, if looking only at the origin spots of the fire rather than the whole region, the pattern of decreasing FMI is consistent.

3.1.3. Normalized Burn Ratio and Burn Severity

The resulting NBR maps (see appendix figures 8-10) show the contrast between the study areas before the fire and after the fire, with the burned area highlighted in the dNBR image. The burn severity classification (BSC) in figure 4 below shows the extent of burned areas, classified

into burn severity ratings established. Observations of the BSC map exhibit that the forested areas on slopes were burned worse.

While it is noticeable that Keremeos Creek has some unburned regions, the other two fire areas seem to be completely affected by the forest fires. The histograms, in graph set 3, skew right for each fire and show that the severity increased post-fire. The data indicates that White River experienced the most severe fires. However, we cannot say that the fires decreased in severity from 2017 to 2022 because each fire was located in a different area, and because we only studied three fires. Further studies comparing multiple fires in similar areas would present more accurate results.

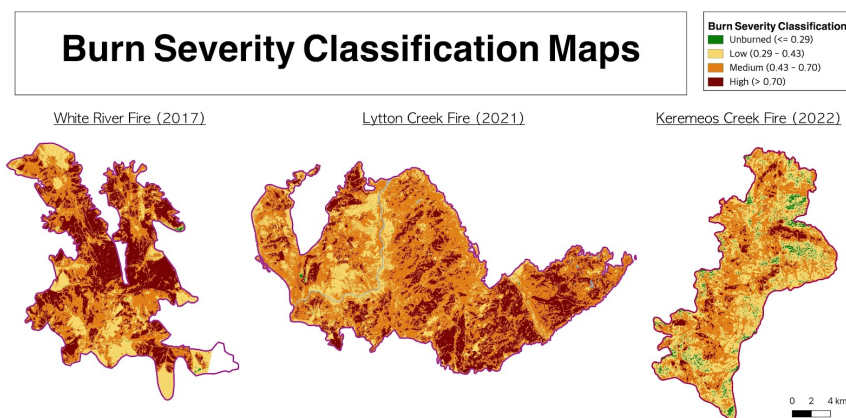


Figure 4. Burn Severity maps for each study year.

3.2. Data validation: Calculating correlation coefficients using Excel

The validation of fire risk variables and burn severity results was attempted using simple linear regression. Finding correlation coefficients (i.e., R^2 values) is a simple, but established statistical method for analyzing the relationships between multiple variables. Using ArcGIS, pixel values were extracted for digital elevation models (DEMs), fuel moisture index (FMI), land surface temperature (LST), and burn severity. This was done for each study fire year, using pre-fire dates. The resulting data was cleaned in Excel by removing pixels with null values. Then, Excel's "Correlation" data analysis function was used for all pixel value sets to calculate correlations between all four factors. Correlation tables were generated for each study year (see appendix table set 1). A summary for each year is in table 2 below.

Year	BS-FMI	BS-LST	BS-DEM	FMI-LST	FMI-DEM	LST-DEM
2017	0.210534	0.014802	0.070889	-0.34926	-0.24549	-0.42376
2021	0.298984	0.061887	-0.05261	-0.18118	-0.31745	-0.45168
2022	0.086542	0.330433	-0.23672	0.118731	-0.68024	-0.50115

Table 2. Correlation coefficients for burn severity, LST, FMI, and slope for each study year.

R^2 values involving burn severity and other variables were positive for each year. However, the majority of R^2 values involving burn severity were smaller than 0.1 and -0.1. Correlation coefficient values range from -1 to 1, so these near-zero values indicate no correlations between burn severity and slope, FMI, or LST. In White River (2017) and Lytton (2021), there was a small negative correlation between FMI and LST (-0.34 and -0.18, respectively), but a small *positive* correlation appeared in Keremeos Creek (2022) (0.18). The negative correlations suggest that fuel moisture decreased and temperature increased before the 2017 and 2021 fires. The positive correlation suggests that fuel moisture

increased and temperature decreased before the 2022 fire. This could be explained by the relatively higher average elevation and vegetation-to-settlement ratio of Keremeos Creek. Weather and climate are other possible factors: the 2017 and 2021 fire incidents both occurred during unprecedented heat waves, and there could have been increased precipitation in the days prior to the 2022 fire.

The FMI-DEM correlations were negative in all 3 years, ranging from -0.24 to -0.68, indicating that moisture decreased with increases in slope. This result supports the qualitative analysis for FMI in 3.1.2 and burn severity in 3.1.3, which suggested that drier leeward slopes were more susceptible to stronger wildfire burn. Another consideration is the role of slopes and water drainage; steeper slopes generally increase moisture gradients from high to low elevations. The LST-DEM correlations from 2017 to 2022 were all negative and ranged from -0.42 to -0.50. These results support findings in the literature review that suggest that surface temperature decreases with slope. Overall, these correlations support the qualitative analysis and literature review suggesting that drier and warmer slopes are more fire-susceptible.

Many factors could have affected validation accuracy. Given the small project sample size, and even smaller temporal sample size (one year), the results are not robust. Additionally, the variables used to calculate correlation values were from different days because of the satellite image sources. For example, the 2017 FMI raster used Sentinel 2 data from July 24, but the LST data was from Landsat 9, on July 25. This project produced validation values suggesting that drier, sloped, and warmer areas are more susceptible to wildfire risk; however, more research using more accurate and precise inter-variable validation methods will yield stronger results.

3.3. Summary of results

This project produced four results:

1. A simple method to compare, analyze, visualize burned area extent and severity within BC using remote sensing imagery.
2. A method to observe trends in fire risk indicators (i.e., fuel moisture, surface temperature, and slope) over time.
3. Tangible burn severity maps that presented fire severity within the study areas.
4. Insights into correlations between fire risk variables and trends in the most recent decade. Findings support literature stating that arid, warm, and sloped conditions increase the likelihood and severity of fires. This could inform or support aerial wildfire management.

3.4. Future Insights

Given some patterns recognized from the data processing and results, future research could devise more detailed workflows for comparing multiple variables, such as random forest regression. Moreover, we propose the idea of implementing a fire forecasting system for BC by monitoring the fire risk variables, which could prove useful in future forest fire prevention.

There are many existing Forest Fire Monitoring Systems that provide information on active forest fires. However, most of these systems use satellite sensors to detect hotspots of fires that have already been ignited. There exists no such system, in British Columbia at least, that maps areas susceptible to a fire for careful observations.

Figure 11 in the Appendix, shares a promising blueprint of a real time monitoring system of forest fire variables that could be adapted into the province's fire management department, B.C. Wildfire Services.

If the fuel moisture content and land surface temperature can be monitored regularly, along with other potential fire risk factors, any concerning variations in these factors during the BC fire season can be identified and the location can be kept under supervision for potential fire risks.

3.5. Limitations

To our knowledge, there is currently no research that focuses on our study area and timeframe. It will provide a rudimentary remote sensing methodology to refine and apply elsewhere as newer fire data and remote sensing methods become available. This includes working with data of higher spatial resolution with smaller temporal extents.

Our literature review discusses studies with more robust, accurate, and useful methods, models, and algorithms; however, we did not reconstruct these methods as they were beyond the scope and expertise of a fourth-year remote sensing course. Thus, there is much potential to apply more complex and accurate remote sensing research and analysis to other wildfires in the province.

4. Summary

This project used remote sensing methodologies to quantity burn severity and analyze fire risk variables by using three recent fires in BC. It fills a literature gap by studying two of BC's prominent wildfire regions within the last half-decade. Findings and generated burn severity maps add to emerging literature about climate change, wildfire activity, and fire forecasting. The methodologies can be applied to wildfires from other locations and times. Results and methodologies can also be used to inform aerial fire management strategies, which can help reduce adverse impacts on ecosystems, communities, economies, and public health.

References

- Adelabu, S. A., Adepoju, K. A., & Mofokeng, O. D. (2020). Estimation of fire potential index in mountainous protected region using remote sensing. *Geocarto International*, 35(1), 29-46. <https://doi.org.proxy.lib.sfu.ca/10.1080/10106049.2018.1499818>
- BC Wildfire Service. (n.d.). *Fire Centres—Province of British Columbia*. Province of British Columbia. Retrieved October 13, 2022, from https://www2.gov.bc.ca/gov/content/safety/wildfire-status/about-bcws/fire-centres#kamlo_ops
- British Columbia. (2010). *The State of British Columbia's Forests*. British Columbia Ministry of Forest, Mines and Lands. https://www2.gov.bc.ca/assets/gov/environment/research-monitoring-and-reporting/reporting/envreportbc/archived-reports/sof_2010.pdf
- British Columbia. (n.d.). *Wildfire Averages - Province of British Columbia*. Gov.bc.ca. <https://www2.gov.bc.ca/gov/content/safety/wildfire-status/about-bcws/wildfire-statistics/wildfire-averages>
- Burt, W. (2015). *Burn Severity Mapping: Differenced Normalized Burn Ratio Burned Area Reflectance Classification*. Government of British Columbia. https://www.for.gov.bc.ca/ftp/rsi/external/!publish/Forest%20Health/Forest%20Health%20Presentations/Fire%20mitigation/2_Will%20Burt_Burn%20Severity%20Mapping_FH-2015_Nelson.pdf
- EOS. (2022). *Normalized Difference Moisture Index: Equation And Interpretation*. Eos.com. <https://eos.com/make-an-analysis/ndmi/>
- Filipponi, F. (2019). Exploitation of Sentinel-2 Time Series to Map Burned Areas at the National Level: A Case Study on the 2017 Italy Wildfires. *Remote Sensing*, 11(6), 622. <https://doi.org/10.3390/rs11060622>
- Haider, W., Knowler, D., Trenholm, R., Moore, J., Bradshaw, P., & Lertzman, K. (2019). Climate change, increasing forest fire incidence, and the value of visibility: evidence from British Columbia, Canada. *Canadian Journal of Forest Research*, 49(10), 1242–1255. <https://doi.org/10.1139/cjfr-2018-0309>
- Leblon, B., Bourgeau-Chavez, L., & San-Miguel-Ayanz, J. (2012). Use of Remote Sensing in Wildfire Management. In (Ed.), Sustainable Development - Authoritative and Leading Edge Content for Environmental Management. IntechOpen. <https://doi.org/10.5772/45829>
- Rittmaster, R., Adamowicz, W. L., Amiro, B., & Pelletier, R. T. (2006). Economic analysis of health effects from forest fires. *Canadian Journal of Forest Research*, 36(4), 868–877. <https://doi.org/10.1139/x05-293>

Santos, S. M. B. dos, Bento-Gonçalves, A., Franca-Rocha, W., & Baptista, G. (2020). Assessment of Burned Forest Area Severity and Postfire Regrowth in Chapada Diamantina National Park (Bahia, Brazil) Using dNBR and RdNBR Spectral Indices. *Geosciences*, 10(3), 106. <https://doi.org/10.3390/geosciences10030106>

Schoennagel, T., Balch, J. K., Brenkert-Smith, H., Dennison, P. E., Harvey, B. J., Krawchuk, M. A., Mietkiewicz, N., Morgan, P., Moritz, M. A., Rasker, R., Turner, M. G., & Whitlock, C. (2017). Adapt to more wildfire in western North American forests as climate changes. *Proceedings of the National Academy of Sciences*, 114(18), 4582–4590. <https://doi.org/10.1073/pnas.1617464114>

Schneider, P., Roberts, D.A., Kyriakidis, P.C. (2008). A VARI-based relative greenness from MODIS data for computing the Fire Potential Index. *Remote Sensing of Environment*. 111(3), 1151-1167. <https://doi.org/10.1016/j.rse.2007.07.010>.

Wang, X., Thompson, D. K., Marshall, G. A., Tymstra, C., Carr, R., & Flannigan, M. D. (2015). Increasing frequency of extreme fire weather in Canada with climate change. *Climatic Change*, 130(4), 573–586. <https://doi.org/10.1007/s10584-015-1375-5>

White, J. C., Wulder, M. A., Hermosilla, T., Coops, N. C., & Hobart, G. W. (2017). A nationwide annual characterization of 25 years of forest disturbance and recovery for Canada using Landsat time series. *Remote Sensing of Environment*, Volume 194, 303-321. <https://doi.org/10.1016/j.rse.2017.03.035>

Appendix



Figure 5. Model for NBR & dNBR processing designed in QGIS' graphical modeler.

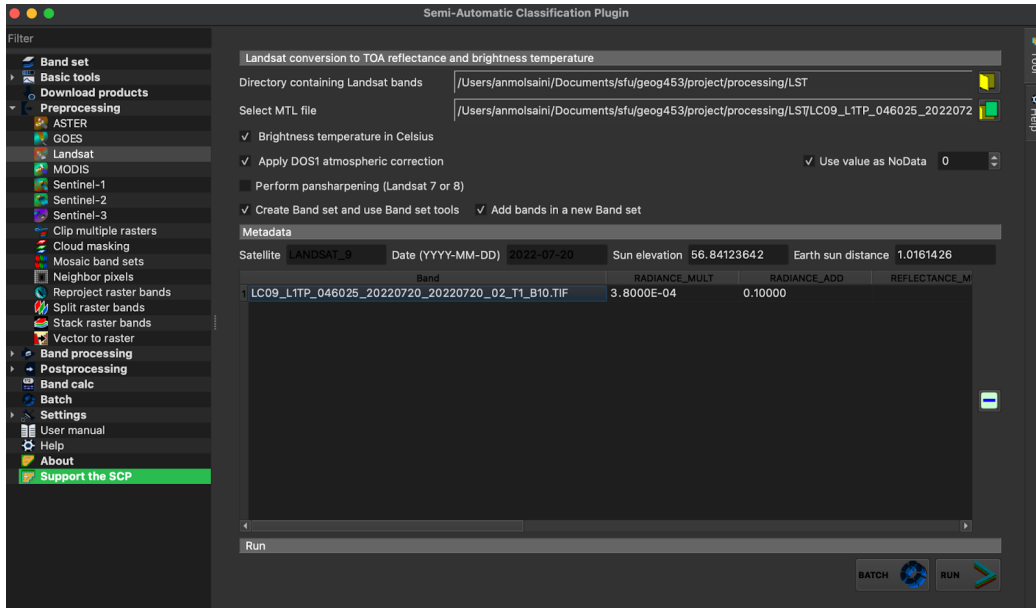


Figure 6. Screenshot of QGIS' Semi-Automatic Classification Plugin used for converting thermal bands to LST.

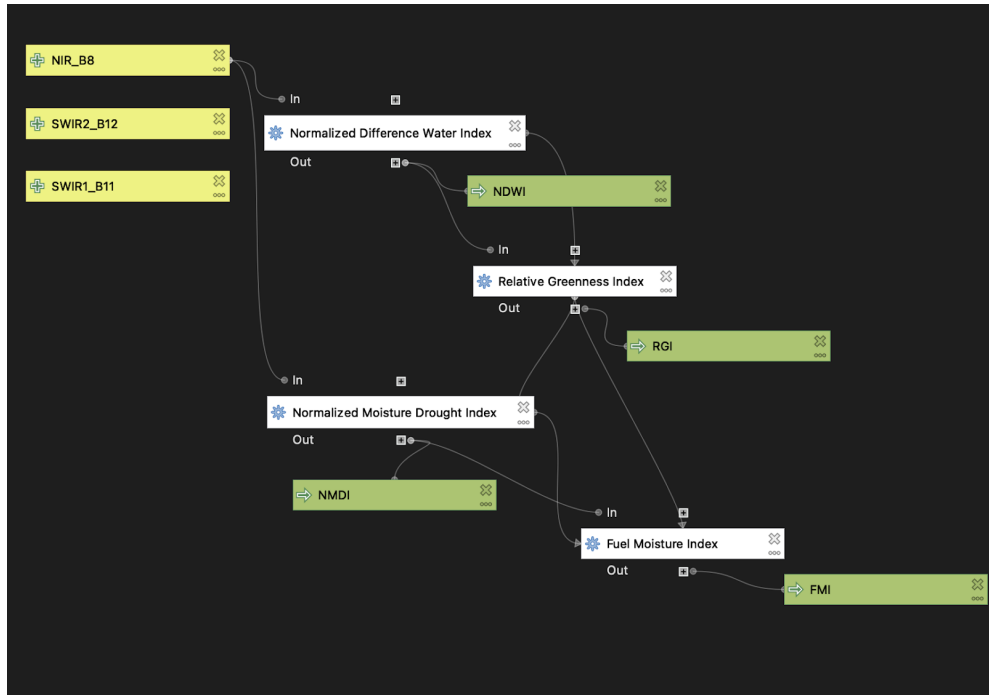


Figure 7. Model for FMI processing designed in QGIS' graphical modeler.

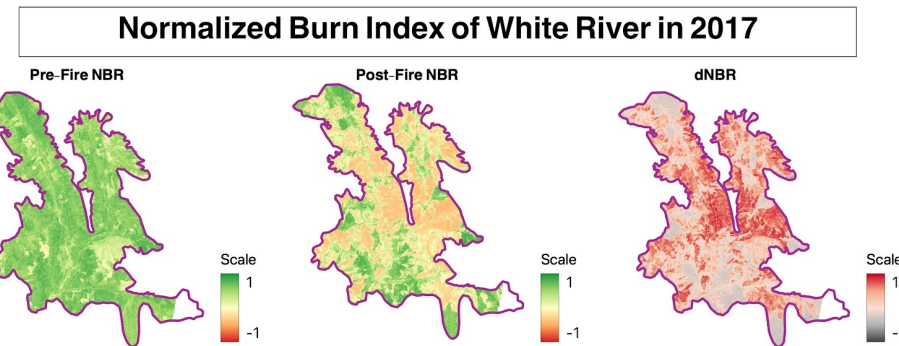


Figure 8. pre-fire NBR, post-fire NBR, and dNBR of White River Fire.

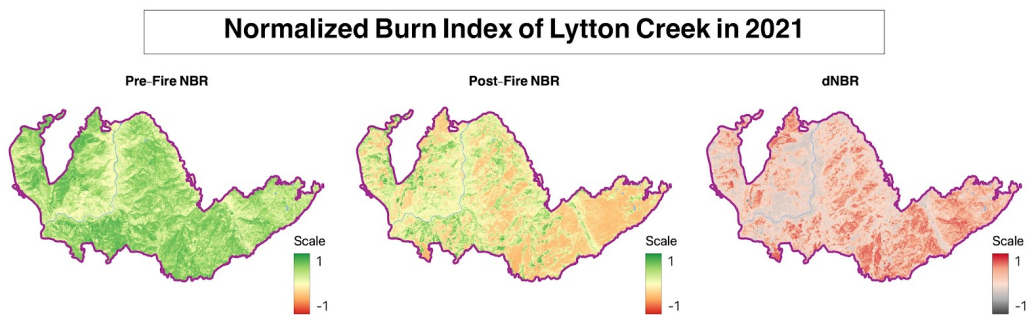


Figure 9. pre-fire NBR, post-fire NBR, and dNBR of Lytton Creek Fire.

Normalized Burn Index of Keremeos Creek in 2022

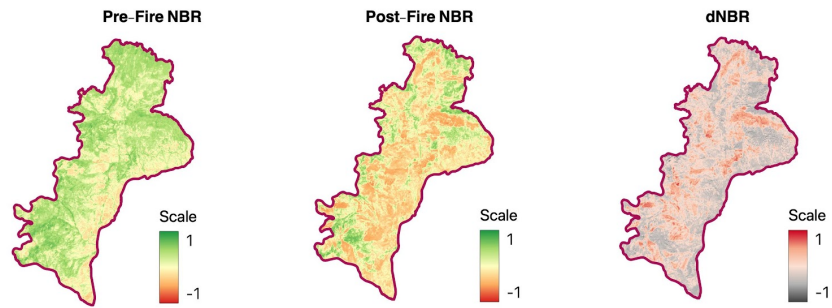
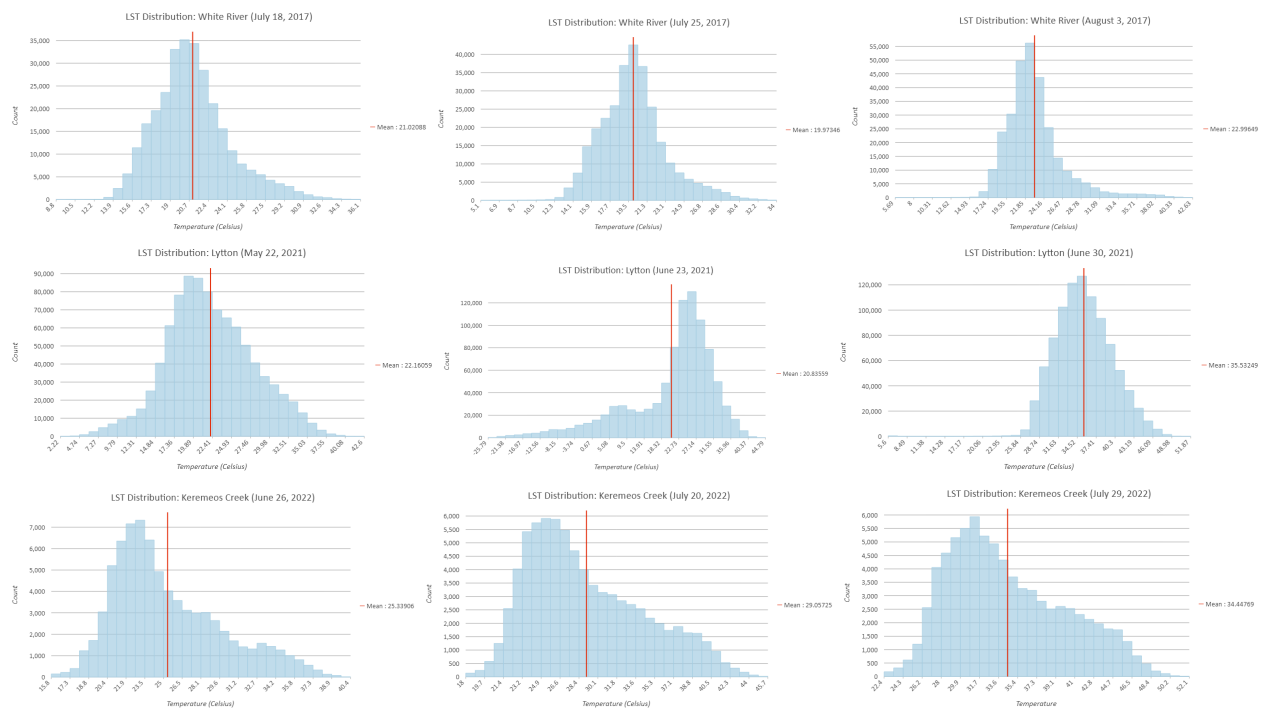
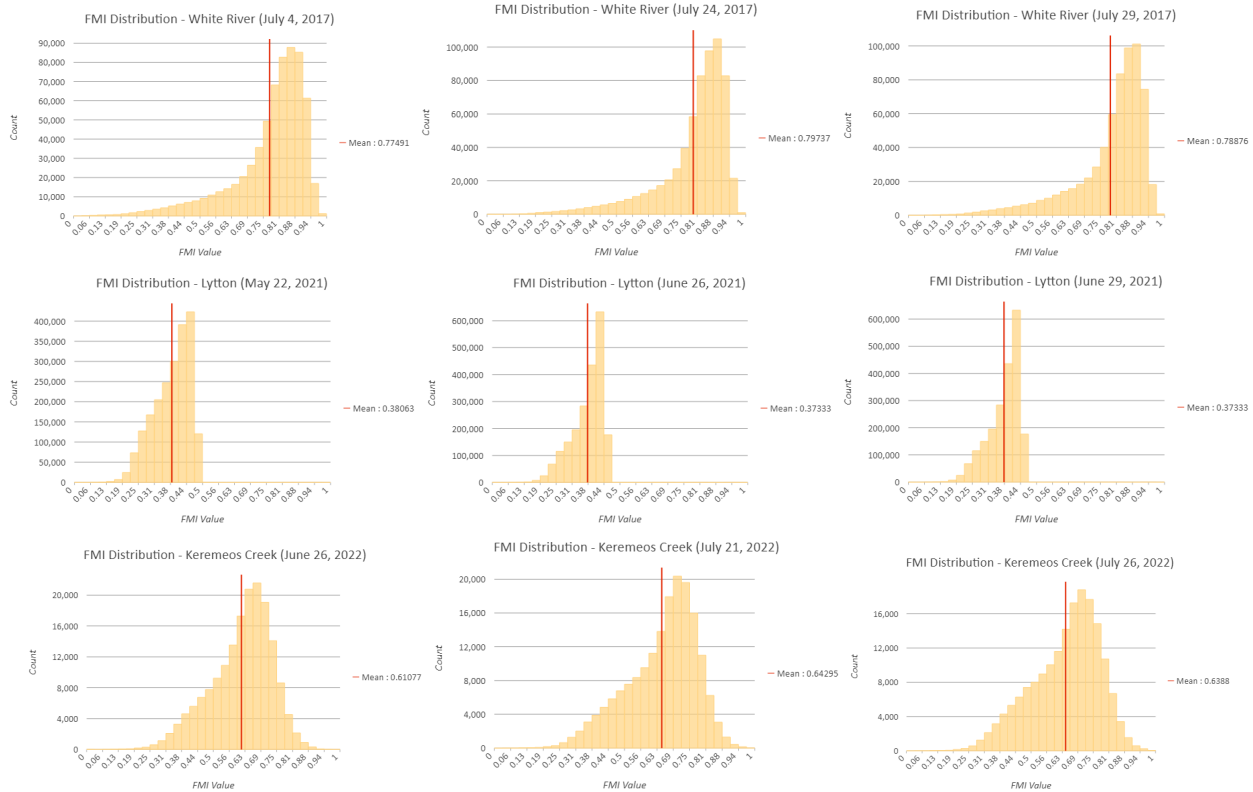


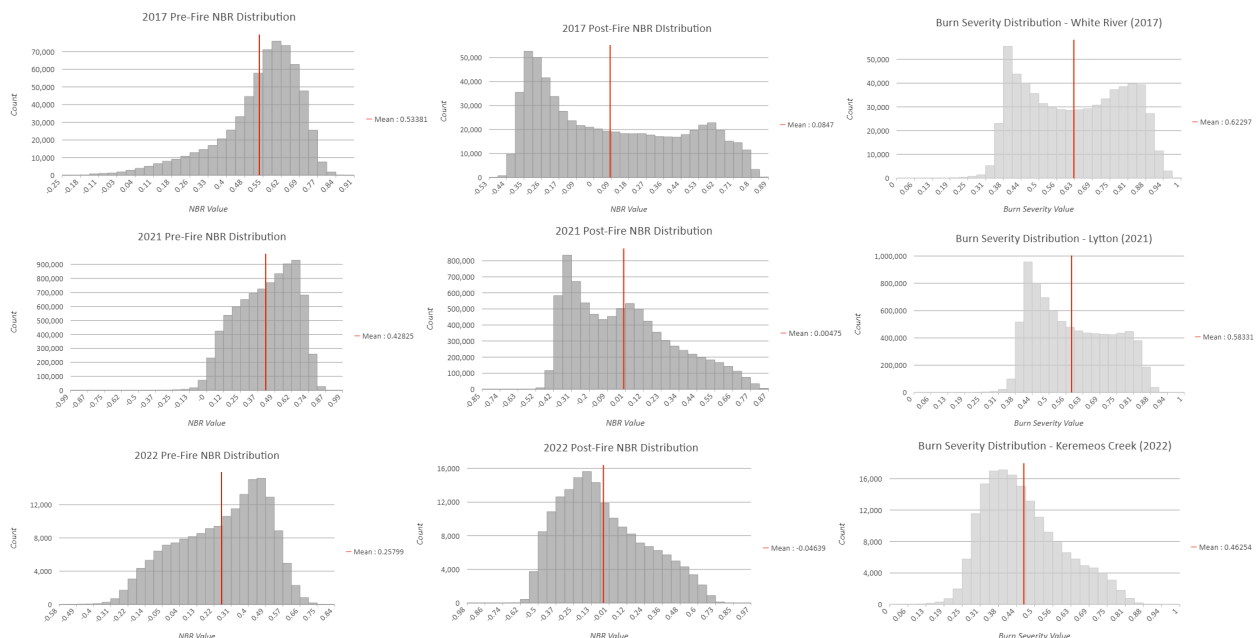
Figure 10. pre-fire NBR, post-fire NBR, and dNBR of Keremeos Creek Fire.



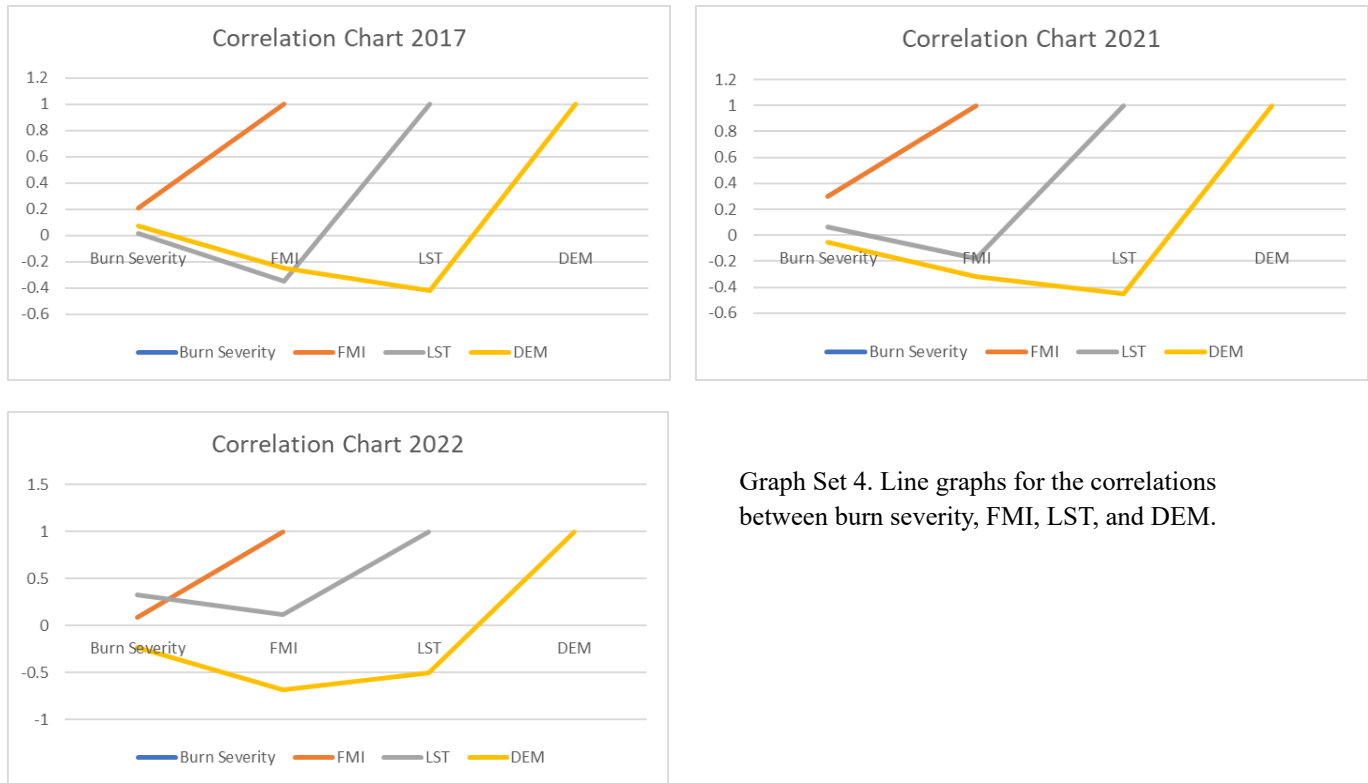
Graph Set 1. Histograms depicting the LST distribution for each fire from Figure 2. (Zoom in to see clearly)



Graph Set 2. Histograms showing FMI distributions for each fire from Figure 3. (Zoom in to see clearly)



Graph Set 3. Histograms depicting the pre-fire NBR, post-fire NBR, and Burn Severity distributions for each fire from Figure 4, 8-10. (Zoom in to see clearly)



Graph Set 4. Line graphs for the correlations between burn severity, FMI, LST, and DEM.

White River 2017	Burn Severity	FMI	LST	DEM
Burn Severity	1			
FMI	0.210534	1		
LST	0.014802	-0.34926	1	
DEM	0.070889	-0.24549	-0.42376	1

Lytton 2021	Burn Severity	FMI	LST	DEM
Burn Severity	1			
FMI	0.298984	1		
LST	0.061887	-0.18118	1	
DEM	-0.05261	-0.31745	-0.45168	1

Keremeos Creek 2022	Burn Severity	FMI	LST	DEM
Burn Severity	1			
FMI	0.086542	1		
LST	0.330433	0.118731	1	
DEM	-0.23672	-0.68024	-0.50115	1

Table 3. Set of tables showing coefficient correlations between burn severity, FMI, LST, and slope for each study fire.

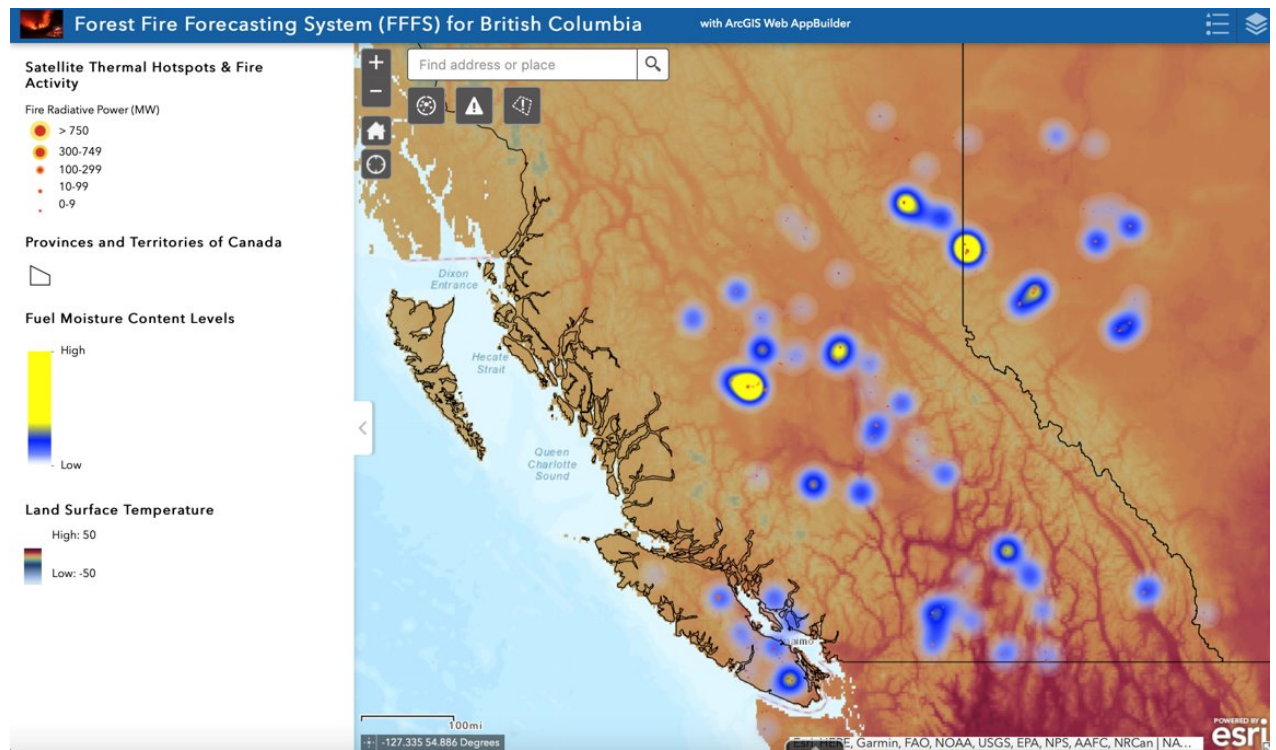


Figure 11. Prototype of a potential Forest Fire Forecasting System that can be implemented by the Government.

(Created in ArcGIS WebApp Builder.)